Supplementary

Table S1. Ice layers suspected to be had impacted by volcanic events

Ice layers	Depth (m)	Depth (mwe)	Volcanic event (A5)	Volcanic event (A3 & A4)
(a)	140.0	106.9	1877/78 Cotopaxi ?	1872 Sinarka, 1872 Merapi, 1972 Vesuvius, 1873 Grimsvotn, 1875 Askja, 1877 Cotopaxi, ???
(b)	146.38	112.57		1854 Shiveluch
(c)	149.16	115.03	1854 Shiveluch ?	1835 Cosigüina ?
(d)	153.70	118.96	1835 Cosigüina	1815 Tambora
(f)	154.73	119.84		
(e)	160.40	124.71		1783 Laki

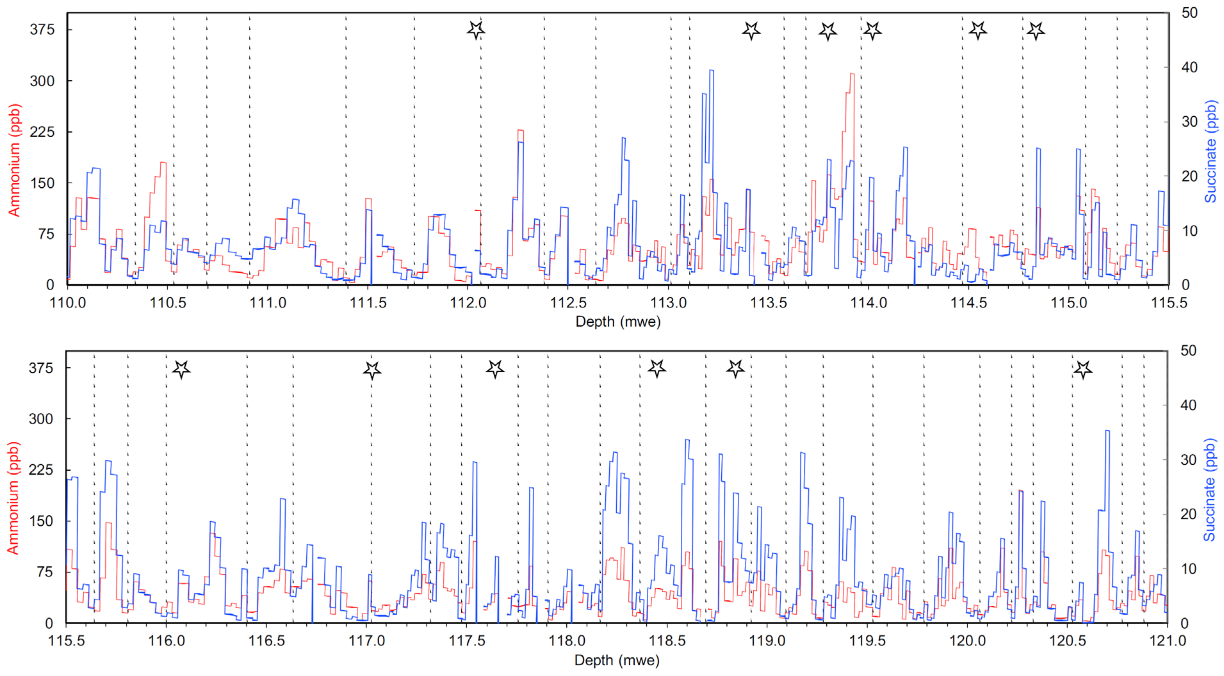

S1 Annual layer counting between 110 and 121 mwe from co-authors A5 and A3. Vertical dashed lines denote yearly dissection proposed by co-author A5 based on identification of winter layers characterized by low concentrations of ammonium and succinate. Stars indicate where co-author A3 counted additional years with respect to those counted by co-author A5.

In the following we evaluate in the extent to which the different dating are consistent with volcanic horizons and from that estimate dating uncertainties. As seen in Figure 2, below the Katmai horizon layer seen at 87.75 mwe, 5 layers (a to e) exhibit sulfate level exceeding 500 ppb together with acidity above 5 µEq L^{-1}. In addition, the layer (f) also revealed an acidity higher than 5 µEq L^{-1} whereas the sulfate level remained below 500 ppb. As seen in Table S1, we attributed layer (b) located at 112.57 mwe (dated at 1851) to the 1854 Shiveluch eruption (Kamchatka) of which the volcanic exclusivity index (VEI) was of 5 (Simkin & Siebert, 1994). Several candidates can explain the layer (a) located at 106.9 mwe (dated at 1874) including 1872 eruptions of Sinarka (Kurile Islands, VEI = 4) and Merapi (Java, VEI = 4), the 1873 eruption of Grimsvotn (Iceland, VEI = 4), the 1875 eruption of Askja (Iceland, VEI = 4), and the 1877 eruption of Cotopaxi (Ecuador, VEI = 4) as well as 1972 eruption of Vesuvius (Italy, VEI=3) located 2500 km to the west of Mt. Elbrus. For the layer (c) located at 115.03 mwe (dated at 1842) we only identify the 1835 Cosigüina eruption (Nicaragua, VEI = 5) as possible candidate. It is, however, difficult to reconciliate the dates of layer b (1851) and c (1842) and identify 22 years between them. The series of spikes located between 118 and 120 mwe was previously identified as possibly related to the 1835 Cosigüina eruption are now attributed to the 1815 Tambora eruption. It remains unclear, however, which layer (d dated at 1817 or f dated at 1813) corresponds to the 1815 Tambora eruption. Further studies including tephras analysis would here help to conclude. Finally, the layer (e) dated at 1789 may be related to the 1783 Laki eruption.

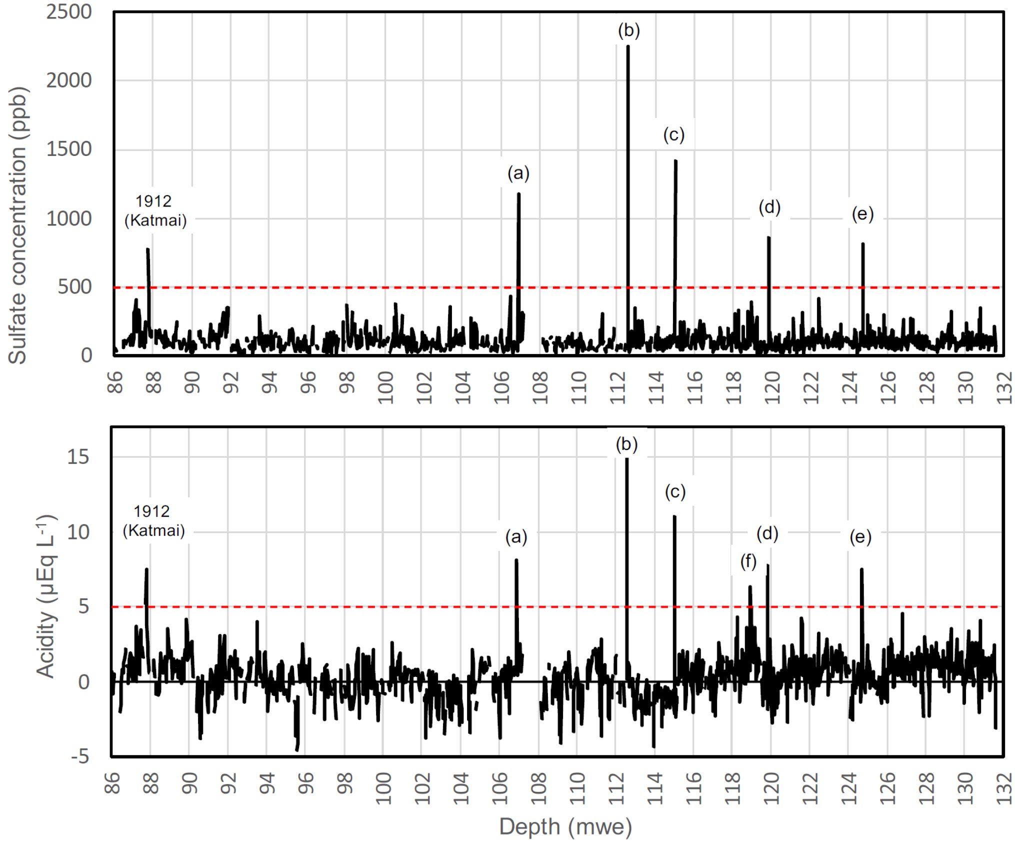

S2. Raw profiles of sulfate and acidity in the Elbrus ice between 86 and 132 mwe. Samples considered to be impacted by large dust events has been removed (see Preunkert et al., 2019). In addition to the 1912 Katmai volcanic horizon at 87.75 mwe, several ice layers revealed sulfate concentrations exceeding 500 ppb (denoted (a) to (e)), and acidity higher than 5 µEq L^{-1} (denoted (a) to (f)) that would be related to other volcanic events (see Table 1). The horizontal red dashed lines indicate the sulfate concentration limit of 500 ppb, the acidity limit of 5 µEq L^{-1}.

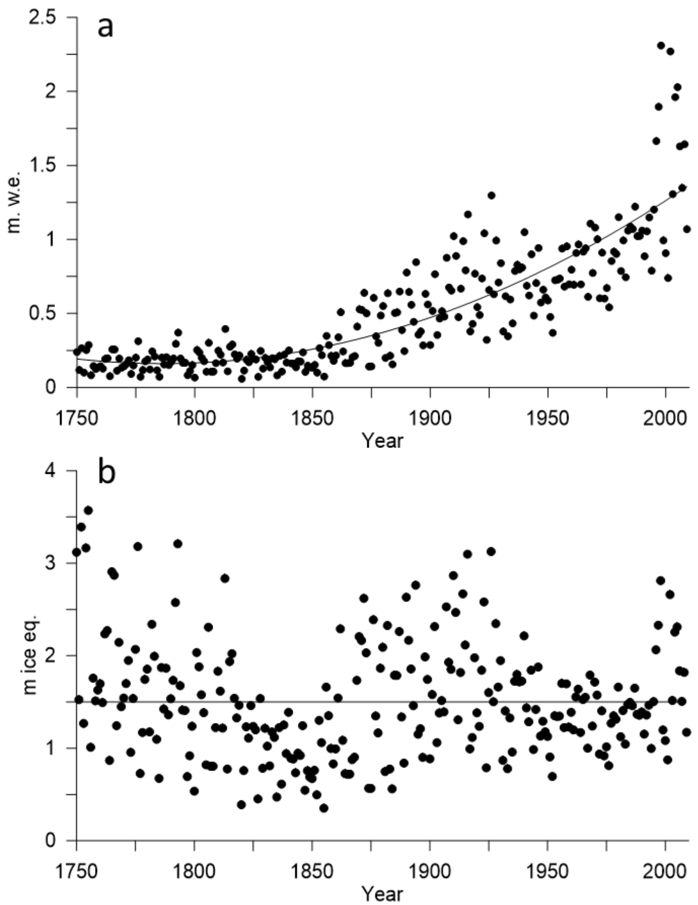

S3. Measured annual layer thickness in ice equivalent (a) and annual layer thickness corrected by the model of J. Nye (Dansgaard and Johnsen, 1969) (b)

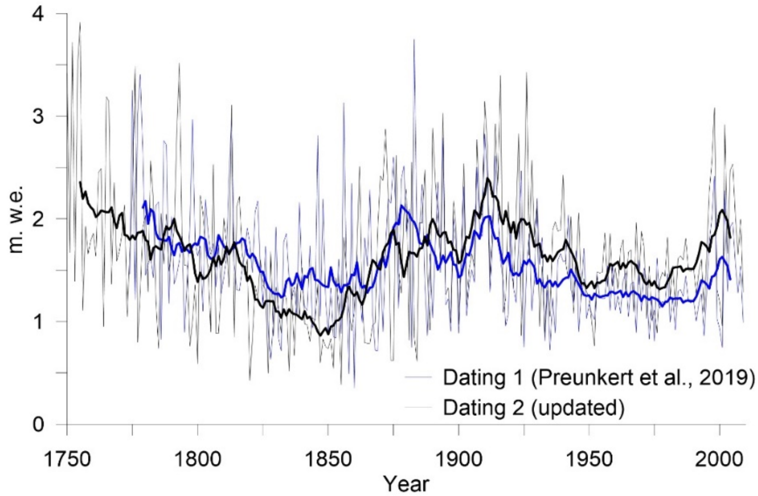

S4 Reconstruction of annual snow accumulation at the WP using different dating (section 2.2.1). 10-year moving averages are shown in thick lines.

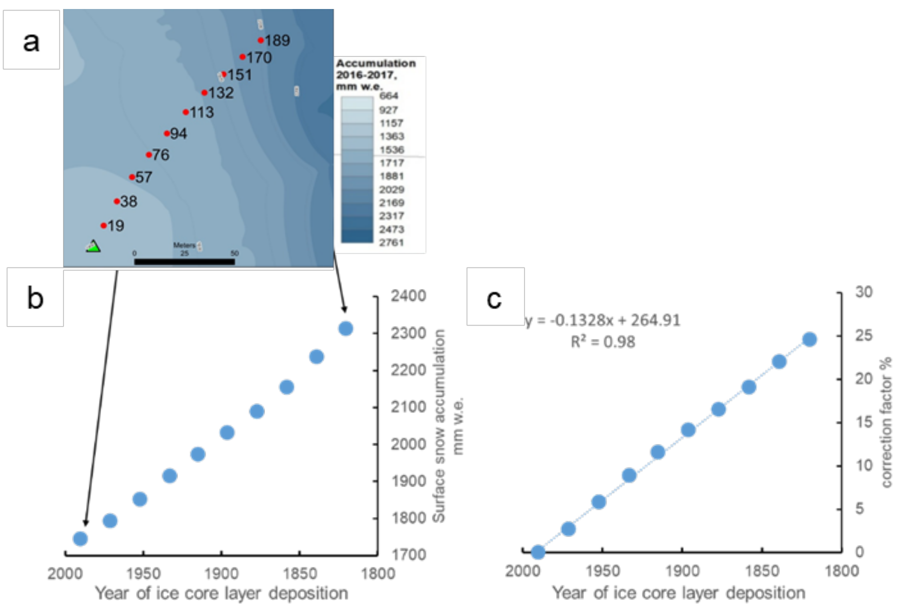

S5 Surface snow accumulation distribution in 2016-2017 (Lavrentiev et al., 2022) (a), surface snow accumulation corresponding to age when the ice core layer was deposited on the glacier surface (b); correction factor to account for the surface accumulation distribution.

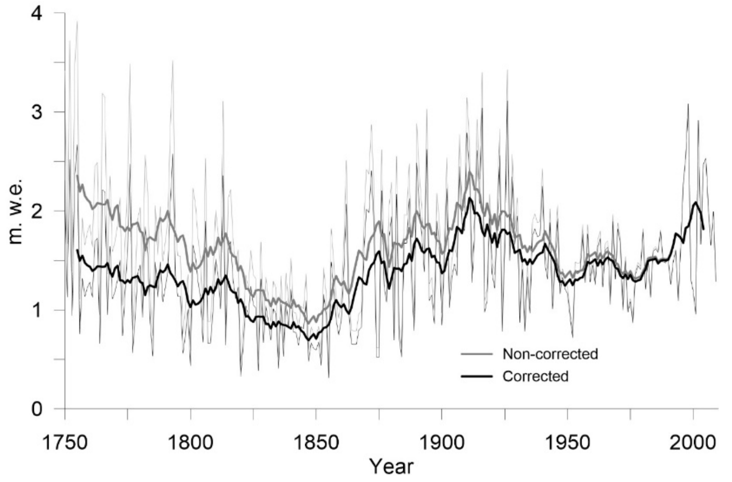

S6 Reconstruction of annual snow accumulation at the WP non-corrected and corrected for snow accumulation surface distribution (section 2.3.2)

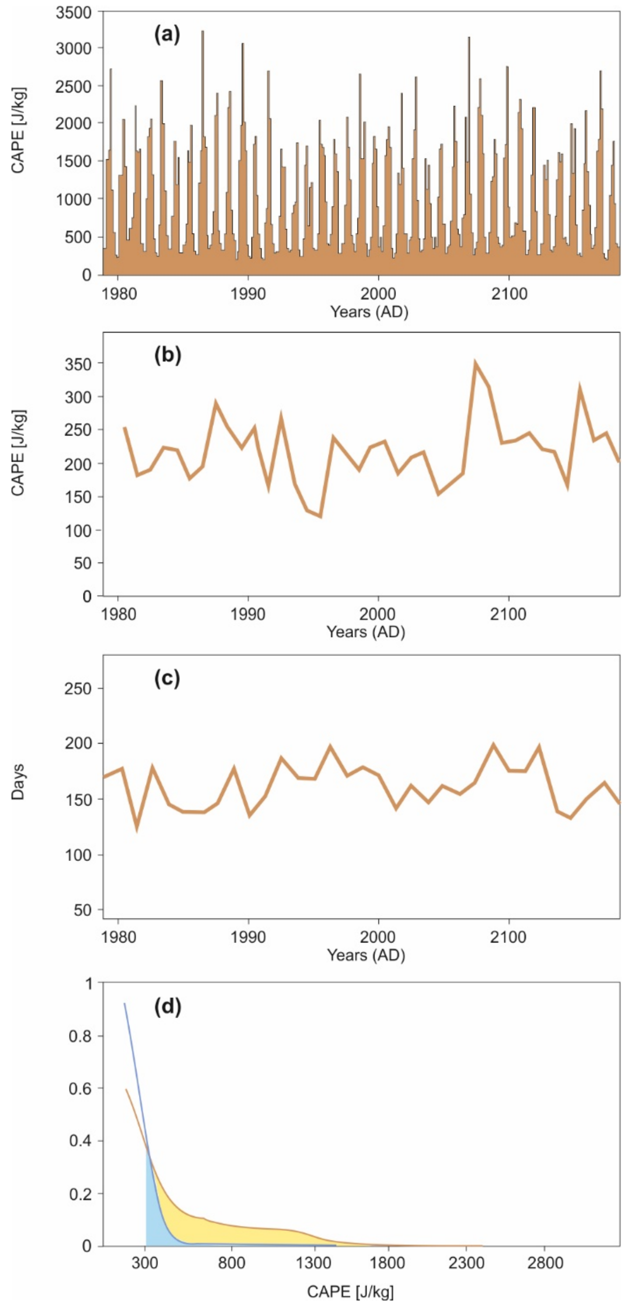

S7. Characteristics of CAPE in the Elbrus region for the period 1979 - 2017 according to CFSR reanalysis data: a) time course in 6-hour steps, b) average values for the warm half-year (May - September), c) number of days with CAPE >300 Jkg^{-1} for each year, d) empirical distribution function of CAPE in winter (November - March) and summer (May - September), colored areas correspond to the total proportion of CAPE >300 Jkg^{-1}, which in cold half-year is 7%, and in warm 40%

Table S8 Seasonal calendar at WP calculated using CAPE

Summer		Winter	
from	to	from	to
12.05.1979	16.10.1979	17.10.1979	09.04.1980
10.04.1980	03.10.1980	04.10.1980	08.05.1981
09.05.1981	25.10.1981	26.10.1981	21.04.1982
22.04.1982	16.10.1982	17.10.1982	17.05.1983
18.05.1983	23.09.1983	24.09.1983	07.04.1984
08.04.1984	02.10.1984	03.10.1984	27.04.1985
28.04.1985	20.09.1985	21.09.1985	29.04.1986
30.04.1986	16.09.1986	17.09.1986	13.05.1987
14.05.1987	30.09.1987	01.10.1987	18.05.1988
19.05.1988	12.10.1988	13.10.1988	10.04.1989
11.04.1989	06.10.1989	07.10.1989	10.05.1990
11.05.1990	25.09.1990	26.09.1990	15.04.1991
16.04.1991	20.09.1991	21.09.1991	19.04.1992
20.04.1992	25.10.1992	26.10.1992	13.04.1993
14.04.1993	01.10.1993	02.10.1993	08.04.1994
09.04.1994	25.09.1994	26.09.1994	13.04.1995
14.04.1995	30.10.1995	31.10.1995	02.05.1995
03.05.1996	22.10.1996	23.10.1996	22.04.1997
23.04.1997	18.10.1997	19.10.1997	26.04.1998
27.04.1998	16.10.1998	17.10.1998	16.05.1999
17.05.1999	07.10.1999	08.10.1999	13.04.2000
14.04.2000	26.09.2000	27.09.2000	10.05.2001
11.05.2001	06.10.2001	07.10.2001	06.05.2002
07.05.2002	16.10.2002	17.10.2002	26.05.2003
27.05.2003	29.10.2003	30.10.2003	27.04.2004
28.04.2004	10.10.2004	11.10.2004	14.04.2005
15.04.2005	31.10.2005	01.11.2005	06.05.2006
07.05.2006	30.10.2006	31.10.2006	07.05.2007
08.05.2007	30.10.2007	31.10.2007	31.03.2008
01.04.2008	16.10.2008	17.10.2008	28.04.2009
29.04.2009	27.09.2009	28.09.2009	16.05.2010
17.05.2010	29.10.2010	30.10.2010	18.05.2011
19.05.2011	19.10.2011	20.10.2011	25.04.2012
26.04.2012	09.10.2012	10.10.2012	01.05.2013
02.05.2013	25.09.2013	26.09.2013	18.04.2014
19.04.2014	18.10.2014	19.10.2014	27.04.2015

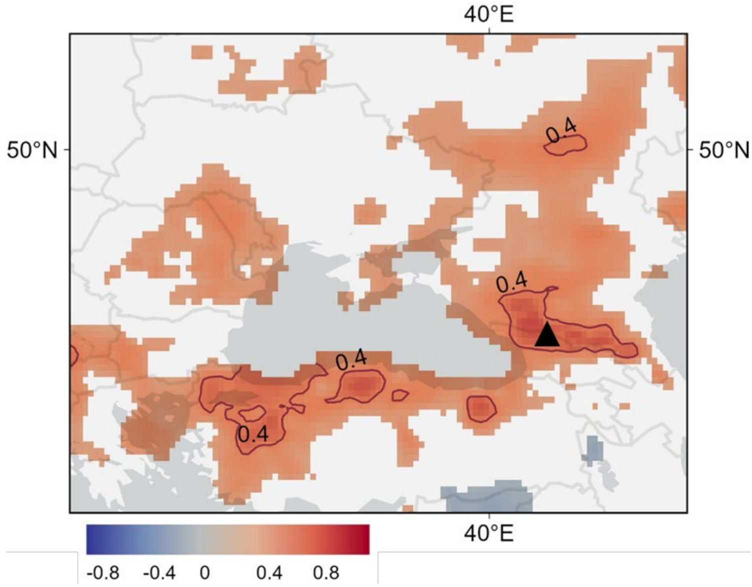

S9. Spatial correlation of the winter WP accumulation with March precipitation data of the GPCC data set in 1950-2009 period.